Chalcogenide Letters Vol. 17, No. 6, June 2020, p. 301 - 313

STRUCTURAL, OPTICAL CONSTANTS AND ENERGY GAP TUNABILITY WHEN INCORPORATING Te INTO CdSe THIN FILM FOR SOLAR CELLS

S. A. ALY[a], D. ABDELMONEM[a], M. ABDEL-RAHMAN[a], E. YOUSEF[b,c], E. R. SHAABAN[d,*]
[a]Physics Department, Faculty of Science, Minia University, Minia, Egypt
[b]Physics Department, Faculty of Science, King Khalid University, P.O. Box 9004, Abha, Saudi Arabia
[c]Research Center for Advanced Materials Science (RCAMS), King Khalid University, Abha 61413, P.O. Box 9004, Saudi Arabia
[d]Physics Department, Faculty of Science, Al-Azhar University, Assiut, 71542, Egypt

In the present work, polycrystalline materials of $CdSe_{1-x}Te_x$ with (x = 0, 0.2, 0.4, 0.6, 0.8 and 1 at. %) were prepared by a conventional solid-state reaction method. Thin films of $CdSe_{1-x}Te_x$ of about 0.5 µm have been produced using evaporation method. The prepared thin films were characterized by using EDAX and X-ray diffractometer. The X-ray diffraction studies shows that the films are polycrystalline in nature, and well oriented along a preferred direction of (002) for hexagonal and along (111) for cubic crystal structure. Both of optical constants (n, k) and film thickness have been determined precisely in terms of envelop method. Analysis of the optical absorption data showed that the transition mechanism takes place by a direct transition. The band gap decreases from 1.677 eV (CdSe) with an increase in Te concentration passing through a minimum of 1.412 eV for $CdSe_{0.4}Te_{0.6}$ (x = 0.6) and then for higher Te concentration band gap increases to 1.486 eV corresponds to pure CdTe. The importance of $CdSe_{1-x}Te_x$ compound is the tunability of band gap when incorporating Te into the CdSe. The dispersion of the refractive index is described using the Wimple–DiDomenico (WDD) single oscillator model. The non-linear refractive index has been discussed.

(Received March 27, 2020; Accepted June 12, 2020)

Keywords: Thin films, $CdSe_{1-x}Te_x$, Optical constants, Swanepoel methods, Linear and nonlinear refractive index

1. Introduction

Both Cadmium telluride (CdTe) and Cadmium Selenide (CdSe) are the two binary compound semiconductors lie in II-VI group. CdTe classified as the most competitive of the thin-film photovoltaics (PV) technologies currently on the market, demonstrating high performance long-term stability and one of the lowest costs [1, 2]. In recent years ternary alloys of these compound semiconductors are potential and interesting candidates in the field of optoelectronic devices. For a long time CdS was considered to be essential in achieving high performance. Solar cells without CdS as a window layer, i.e. CdTe contact directly with the transparent conducting oxide electrode has low open circuit voltages (V_{OC}) and low fill factors (FF), indicating that the CdTe/oxide interfaces were of inferior quality [3, 4]. The essential benefit of CdS is allowing the formation of $CdS_{1-x}Te_x$ and $CdTe_{1-y}S_y$ phases which ease the lattice mismatch at the interface [5]. CdS is limited to performance because has a strong parasitic absorption in the 300–525 nm range (absorption in the CdS does not take part to the photocurrent) [6, 7]. Recently, CdS has been replaced with CdSe layer to share with CdTe because, it has 1.7 eV band gap CdSe that leads to the increasing in optical absorption in this layer, which act to reduce short circuit density (J_{SC}) compared to CdS. It has been demonstrated though that during cell processing the CdSe diffuses into the CdTe, converting it from a photoinactive CdSe (wurtzite) phase to a photoactive $CdTe_{(1-x)}Se_x$ (zincblende) structure [8, 9]. This has the effect of removing the unwanted CdSe layer, and replacing it with a lower band gap $CdTe_{(1-x)}Se_{(x)}$ (≈ 1.36 eV) layer which increases photocurrent

---

[*] Corresponding author: esam_ramadan2008@yahoo.com

compared to CdTe, i.e. cadmium chalcogenides indicate that the band gap of $CdTe_{(1-x)}Se_x$ system can be tuned by varying Se and Te concentration. In addition to a reduction in short wavelength losses [10, 11], photon collection is extended to longer wavelengths. In order to achieve high efficiency multijunction solar cells, controlling of the band gap of the absorber layer is required. i.e. The addition of CdSeTe layers results in the improved current collection at long wavelengths. In the present work, an attempt has been made to grow $CdSe_{(1-x)}Te_{(x)}$ thin films by varying x (0–1) with thermal evaporation method. Optical band gap of CdSeTe alloyed thin films were measured to evaluate material behavior as the tellurium incorporation in the films is increased. This is one of the important semiconductor compounds, as a top device in a high efficiency tandem solar cell structure, due to its tunable physical parameter [12, 13]. Therefore, the aim of this paper is to fully understand the behavior of the optical constants and nonlinear refractive index, furthermore energy gap as a function of composition.

2. Experimental details

Different composition of ternary polycrystalline $CdSe_{1-x}Te_x$ with (x = 0, 0.2, 0.4, 0.6, 0.8 and 1 at. %) were taken in molecular stoichiometric proportional weight of high purity (99.999% produced by Aldrich) analytical grade of ZnTe and CdTe powders according to the following relation:

$$(1-x)CdSe + xCdTe \rightarrow CdSe_{1-x}Te_x \tag{1}$$

At room temperature, the powders were mixed together in a mechanical ball mortar for about 2 hour. After that, the mixed powders were then pressed into a circular disk shape pellet. Such pellets were used as the starting materials from which the thin film will be prepared. The different sets of samples of varying compositions of $CdSe_{1-x}Te_x$ were deposited via evaporation of the compound in vacuum higher than 10^{-6} Pa under controlled growth conditions of various compositions onto the precleaned glass substrates at the temperature of 373 K), using a conventional coating unit **(**Edward 306A**)**. The rate of evaporation thickness of the film thickness were controlled using a quartz crystal DTM 100 monitor. The deposition rate was maintained 20 Å/s constant throughout the sample preparations. The structure of the prepared samples were studied by XRD analysis (Philips X-ray diffractometry (1710)) with Ni-filtered Cu Kα radiation with λ = 0.15418 nm). The intensity data were collected using the step scanning mode with a small interval ($2\theta = 0.05^o$) with a period of 10 s at each fixed value to yield reasonable number of counts at each peak maximum. The compositional analysis of the obtained films was done by energy dispersive X-ray spectrometer (EDXS) unit interfaced to scanning electron microscope (SEM) (Philips XL) operating at an accelerating voltage of 30 kV. The relative error of determining the indicated elements does not exceed 2.2 %. X-ray energy dispersive spectroscopy (EDAX) spectrum checked for both $CdSe_{0.80}Te_{0.20}$ and $CdSe_{0.80}Te_{0.20}$ films are shown in Fig. 1. The representative Cd, Se and Te peaks are clearly seen in the spectrum and no traces of other elements were noticed in the spectra confirming the purity of the samples. . The findings are in good agreement with the chemical composition of the intended to be made sample. It is found that the film is slightly rich in selenium having 81% and 19% for $CdSe_{0.80}Te_{0.20}$ and the film is slightly rich in tellurium having 81% tellurium and 19% selenium for $CdSe_{0.80}Te_{0.20}$. The transmittance (T) and reflectance (R) optical spectra of the deposited films were performed at room temperature using UV–Vis–NIR JASCO–670 double beam spectrophotometer. At normal incidence, the transmittance spectra were collected without substrate in the reference beam in the wavelength range 300–2500 nm, while the reflectance spectra was measured using reflection attachment close to normal incidence (~5^o).

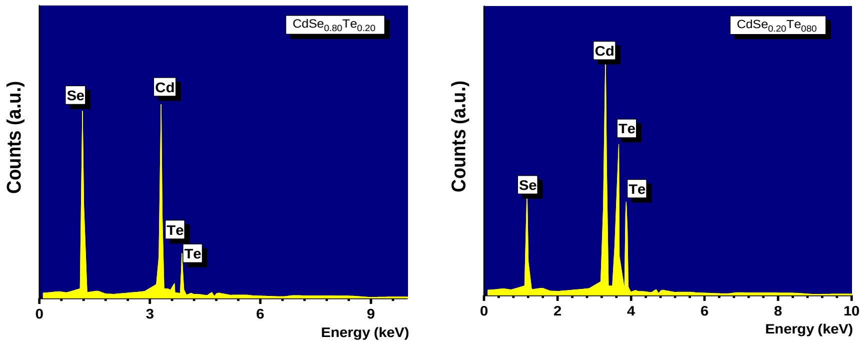

Fig. 1. EDAX of $CdSe_{0.80}Te_{0.20}$ and $CdSe_{0.20}Te_{0.80}$ films.

3. Results and discussion

3.1. Structural properties

In order to understand the structural and electronic level properties of the $CdSe_{1-x}Te_x$ with (x = 0, 0.2, 0.4, 0.6, 0.8 and 1 at. %) thin films onto glass substrate, the crystal structure of the films was studied by X-ray diffraction (XRD) as shown in Fig. 2. This figure shows that the films have good crystallinity. The XRD pattern of the pure CdSe thin films shows a preferential oriented peak (002) at $2\theta = 25.26$ ^{o}C, which is in good agreement with standard (JCPDS # 02-0330), of CdSe powder for hexagonal crystal structure. Similarly, the X-ray diffraction spectra of pure CdTe thin films shows a strong peak at $2\theta = 23.66$ ^{o}C, which corresponds to (111) reflection having cubic zinc blende structure (JCPDS # 01-075-2086). $CdSe_{1-x}Te_x$ compound with x = 0.2 is found to exhibit hexagonal crystal structure with preferred orientation along (002) plane. The film with compositions x = 0.4 and 0.6, both cubic zinc blende and hexagonal wurtzite structures are found to co-exist in the system. for higher concentration with x = 0.8, it goes to cubic structure corresponding to CdTe.

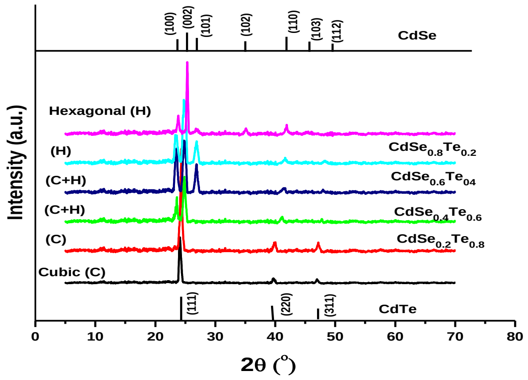

Fig. 2. X-ray diffraction patterns of $CdSe_{1-x}Te_x$ thin films with (x = 0, 0.2, 0.4, 0.6, 0.8 and 1 at. %).

The lattice constant ‘a’ for cubic system can be determined using the following relation [14, 15].

$$a = \frac{d}{\sqrt{h^2 + k^2 + l^2}} \qquad (2)$$

The hexagonal wurtzite crystals are characterized by two lattice parameters, a and c, and the interplanar is given by [14, 15]:

$$\frac{1}{d_{hkl}^{2}}=\frac{4}{3}\frac{h^{2}+hk+k^{2}}{a^{2}}+\frac{l^{2}}{c^{2}} \tag{3}$$

The lattice constants ‘a’ and ‘c’ of the films were calculated from XRD data using the following simple equations

$$a=b=\lambda\left(\sqrt{3}\sin\theta\right)^{-1} \tag{4-a}$$

and

$$c=\lambda\left(\sin\theta\right)^{-1} \tag{4-b}$$

The interplanar spacings d_{hkl} for these thins films were calculated from Bragg's law [16]

$$\lambda=2d_{hkl}\sin\theta \tag{5}$$

where *hkl* are Miller indices of the plane

The lattice parameter values ‘*a*’ for the cubic phase and ‘*a*’ and ‘*c*’ for the hexagonal phase of $CdSe_{1-x}Te_x$ thin films of different compositions have been calculated and their dependence on composition is shown in Table 1.

Table 1. Structural parameters of CdSe1-xTex (x = 0–1) thin films.

Sample	**a(cubic) (Å)**	**a(Hex) (Å)**	**c(Hex) (Å)**	**Crystallize size (nm)**		**Lattice strain (x 10^{-3})**	
				Hex.	**Cub.**	**Hex.**	**Cub.**
CdSe	--	4.29	7.03	45.4	--	1.56	--
$CdSe_{0.8}Te_{0.2}$	--	4.30	7.06	30.3	--	8.66	--
$CdSe_{0.6}Te_{0.4}$	6.12	4.31	7.07	55.2	51.1	5.22	6.23
$CdSe_{0.4}Te_{0.6}$	6.20	4.32	7.08	66.3	67.4	1.21	1.19
$CdSe_{0.2}Te_{0.8}$	6.33	--	--	--	33.5	--	9.24
CdTe	6.44	--	--	--	42.2	--	2.01

Both crystallize size, D_v and lattice strain, ε of $CdSe_{1-x}Te_x$ films are calculated using the following equations [17, 18]

$$D_v=\frac{k\lambda}{\beta\cos(\theta)} \tag{6}$$

and

$$\varepsilon=\frac{\beta}{4\tan(\theta)} \tag{7}$$

where θ represents the Bragg’s angle of the diffracted peak, λ represents the wavelength of CuKα radiation (1.54 Å) and β is the breadth of the diffracted peak, which describes the peak broadening and is determined according to the formula:

$$\beta=\sqrt{\beta_{obs}^{2}-\beta_{std}^{2}} \tag{8}$$

where β_{obs} is the is the breadth of the diffracted peak of the sample and β_{std} is the breadth of the diffracted peak of standard (silicon).

Both D_v and ε are calculated for each phase and listed in Table 1. The change in both D_v and ε may attributed to change in the crystal structure from hexagonal to cubic and associated lattice distortion due to the incorporation of tellurium.

3.2. Optical properties of $CdSe_{1-x}Te_x$ thin films

The transmittance, $T(\lambda)$ and reflectance, $R(\lambda)$ spectra of $CdSe_{1-x}Te_x$ thin films with (x = 0, 0.2, 0.4, 0.6, 0.8 and 1 at. %) are presented in Fig. 3.

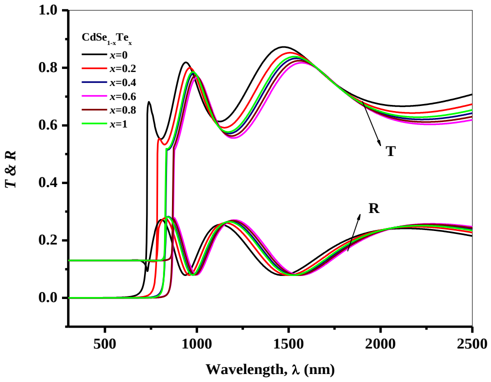

Fig. 3. The transmittance and reflectance spectra of $CdSe_{1-x}Te_x$ thin films with (x = 0, 0.2, 0.4, 0.6, 0.8 and 1 at. %).

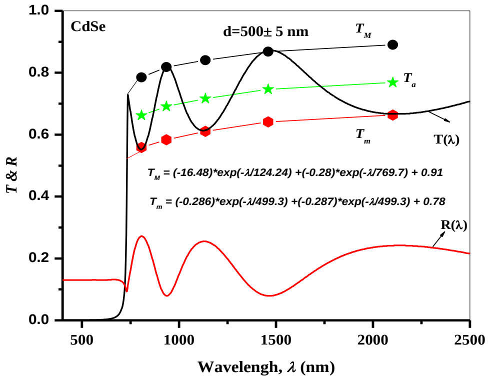

Fig. 4. Variation of envelope construction of the typical spectral transmittance and reflectance vs. wavelength for $CdSe_{1-x}Te_x$ thin film with (x = 0).

Before extracting the optical constants of of the $CdSe_{1-x}Te_x$ with (x = 0, 0.2, 0.4, 0.6, 0.8 and 1 at. %) thin films, the refractive index of their substrate must first be calculated using the following equation [19, 20]:

$$s = \frac{1}{T_s} + \sqrt{\left(\frac{1}{T_s} - 1\right)} \tag{2}$$

where T_s is the transmittance of the glass substrate which has been defined by the polynomial following function:

$$Ts_j = [0.901414\text{-}\{8.02369*10^{-5}[\lambda_j]\} + \{6.13838*10^{-8}[\lambda_j]^2\} - \{1.38877*10^{-11}[\lambda_j]^3\}] \tag{3}$$

where j is integer number refers to specific wavelength.

3.2.2. Envelope construction, refractive index and film thickness

To construct the two envelopes at the extreme points of maximum, and minimum of the interference fringes in the transmission spectrum, we used a appropriate functions which were expressive the two envelopes construction as follows:

$$T_{M_j} = T_0 + A_1 e^{-\frac{\lambda_j}{t_1}} + A_2 e^{-\frac{\lambda_j}{t_2}} \tag{4}$$

$$T_{m_j} = T_0 + A_1 e^{-\frac{\lambda_j}{t_1}} + A_2 e^{-\frac{\lambda_j}{t_2}} \tag{5}$$

where the constants of each equation are different from the other equation constants and vary from one composition to another. Here T_M and T_m are the transmission maximum and the corresponding minimum at a certain wavelength λ. Alternatively, one of these values is an experimental interference extreme and the other one is derived from the corresponding envelope; both envelopes were computer--generated using the program Origin version 7 (Origin-Lab Corp.).

The refractive index of thin film with uniform thickness, n_e in the spectral region of transparent, weak and medium absorption regions can be calculated by the expression [21, 22]:

$$n_1 = \sqrt{N + \sqrt{N^2 - s^2}} \tag{6}$$

where

$$N = 2s\left[\frac{T_{M_j} - T_{m_j}}{T_{M_j} T_{m_j}}\right] + \left[\frac{s^2 + 1}{2}\right] \tag{7}$$

The values of n_e (the refractive index of thin films at extremes interference fringes) were calculated from these equations for all samples and were listed in Table 2.

Table 2. Values of two envelopes T_M and T_m for $CdSe_{1-x}Te_x$ thin films with (x = 0 at. %). The calculated values of refractive index and film thickness are based on the envelope method.

Sample	**λ_e (nm)**	**T_M**	**T_m**	**S**	**n_e**	**d_1**	**m_o**	**m**	**d_2**	**n_2**
CdSe	807.16	0.785	0.558	1.43971	2.384	--	3.015	3	507.75	2.47
	935.51	0.818	0.583	1.44265	2.355	506.54	2.569	2.5	496.54	2.37
	1136.76	0.840	0.610	1.44296	2.295	514.26	2.061	2	495.21	2.28
	1460.12	0.868	0.641	1.43743	2.234	--	1.562	1.5	490.09	2.20
	2102.49	0.890	0.663	1.43664	2.201	--	1.068	1	477.52	2.13

$$\overline{d_1} = 510.40\ nm \quad \sigma_1 = 3.858\ nm (0.756\%) \quad \overline{d_2} = 493.42\ nm$$

$$\sigma_2 = 9.819\ nm (1.1\%)$$

Values of refractive index of thin films, n_1 at any adjacent maximas (or minimas), that have been calculated by Eq. 6, are using to determine the thickness film, d_1. If n_{e1} and n_{e2} are the refractive indices of two adjacent maxima or minima at wavelengths λ_{e1} and λ_{e2}, then the thickness of the film is given by:

$$d_1 = \frac{\lambda_{e1}\lambda_{e2}}{2[\lambda_{e1}n_{e2} - \lambda_{e2}n_{e1}]} \tag{8}$$

where λ_{e1} and λ_{e2} are the wavelengths at any two adjacent maximas (or minimas), and n_{e1} and n_{e2}, are the refractive indices at the corresponding wavelengths. To improve accuracy of thickness film there was a set of order number m_0 for the interference fringes was calculated using equation:

$$m_0 = \frac{2n_{e1}\overline{d_1}}{\lambda_{e1}} \tag{9}$$

where n_{e1} and λ_{e1} are the values taken at the extreme point of the interference fringes and $\overline{d_1}$ is the average of thickness (from Eq. 8), then by taking the approximate value of m_0 produces a new order number m where m = 1, 2, 3... at the maximum points in the transmission spectrum and m = 1/2, 3/2, 5/2... at minimum points in the transmission spectrum after that the accuracy of refractive index in terms of accuracy of thickness thin film expresses as the following formula:

$$n_2 = \frac{m\lambda_{e1}}{2\overline{d}} \tag{10}$$

where $\overline{d}$ is the new average accuracy thickness of thin films after rounded m_0 to m. The final values of new refractive index n_2 and other mentioned values are listed in Table 2.

Fig. 5 shows the dependence the refractive index, n of studied thin films on wavelength, λ. This figure illustrates that the change values of n was related to the change in the concentration of Te to the expense of Se content.

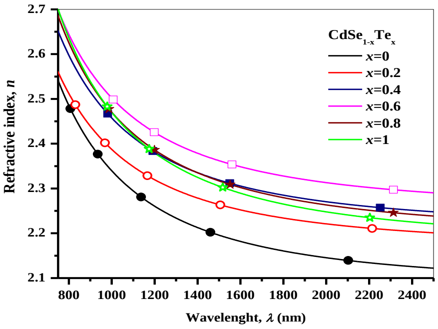

Fig. 5. The spectral dependence of refractive index on wavelength for $CdSe_{1-x}Te_x$ thin films with (x = 0, 0.2, 0.4, 0.6, 0.8 and 1 at. %).

The values of n_2 can be fitted to a reasonable function such as the two-term Cauchy dispersion relationship, which is valid for the thin film model [25, 26]:

$$n_{Cauchy} = a + \frac{b}{\lambda^2} \tag{11}$$

By using the least squares fit, in the two-term Cauchy dispersion relationship; the two sets of values (a, b) of n_2 for studied films are extracted and listed in Table 2.

3.2.3. Determination the absorption coefficient and band gap energy

The absorption coefficient α can be obtained in the strong absorption region of the experimentally measured values of $R(\lambda)$ and $T(\lambda)$ according to the following expression [27, 28]

$$\alpha = \frac{1}{d}\ln\left[\frac{(1-R)^2+\sqrt{\{(1-R)^4+4R^2T^2\}}}{2T}\right] \qquad (13)$$

where d (cm) is the film thickness. Fig. 5 shows the dependence of the absorption coefficient α on the incident photon energy ($h\nu$) for $CdSe_{1-x}Te_x$ with (x = 0, 0.2, 0.4, 0.6, 0.8 and 1 at. %) thin films. For the intermediate region between cubic and hexagonal crystal structure phases are observed, absorption feature represents an average of the two phases. The optical band gap was determined from absorption spectra of the films in the high absorption region ($\alpha > 10^4$ cm^{-1}) using the following relationship [29-31],

$$(\alpha.h\nu) = A(h\nu - E_g)^r \qquad (14)$$

where A is a constant that depends on the transition probability, E_g is the optical energy gap of the material and r is a number which characterizes the transition process, having a value 1/2 for the direct allowed transition and value of 2 for the indirect transition. Linear nature in the plots indicates direct band gap nature of prepared thin films.

We plotted $(\alpha.h\nu)^2$ and $(\alpha.h\nu)^{1/2}$ vs. ($h\nu$) for $CdSe_{1-x}Te_x$ thin films (as shown in Fig. 6 and Fig. 7) and the best linear fitting was taken at for m = 2 confirming an allowed direct transition as illustrated in Fig. 6. The intercept of the extrapolation fitting line with the abscissa (energy axis) would give the E_g^{opt} . The band gap values are tabulated in Table 3. The variation of band gap with CdTe concentration is shown in Fig. 8.

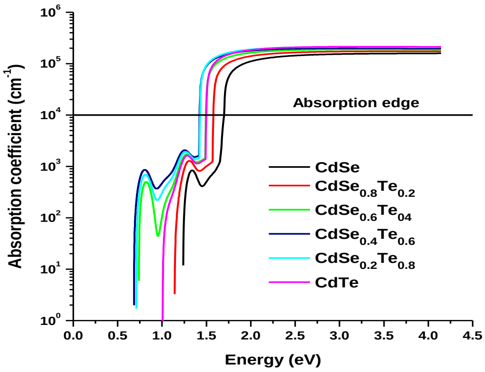

Fig. 6. The absorption coefficient vs. photon energy for $CdSe_{1-x}Te_x$ thin films with (x = 0, 0.2, 0.4, 0.6, 0.8 and 1 at. %).

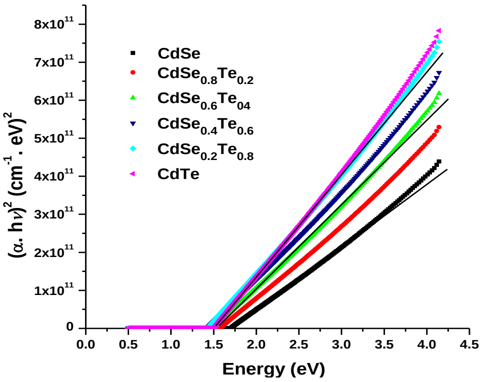

Fig. 7. The plot of $(\alpha.h\nu)^2$ vs. photon energy for $CdSe_{1-x}Te_x$ thin films with (x = 0, 0.2, 0.4, 0.6, 0.8 and 1 at. %).

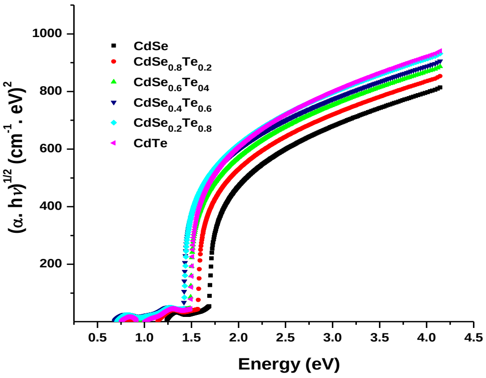

Fig. 8. The plot of $(\alpha.h\nu)^{0.5}$ vs. photon energy for $CdSe_{1-x}Te_x$ thin films with (x = 0, 0.2, 0.4, 0.6, 0.8 and 1 at. %).

The band gap decreases from 1.677eV (CdSe) with an increase in Te concentration passing through a minimum of 1.412eV for $CdSe_{0.4}Te_{0.6}$ (x = 0.6) and then for higher Te concentration band gap increases to 1.486 eV corresponds to pure CdTe. It is observed that the variation in the band gap with composition exhibits band gap bowing in a quadratic form. Similar band gap bowing behavior in $CdSe_{1-x}Te_x$ system was reported by several workers [32-34]. The relationship between optical bandgap and alloy composition can be expressed using the standard bowing equation

$$E_g(x) = bx(1-x) + \left[E_{g(CdTe)} - E_{g(CdSe)}\right]x - E_{g(CdTe)}$$

here $E_{g(CdTe)}$ and $E_{g(CdSe)}$ are the bulk bandgaps of CdTe and CdSe, respectively and b is the optical bowing parameter. Unmatching of the electro-negativity of anions like Te & Se playing an important role in the bowing of band gap that was explained by Nacir Tit et al., [35] using theoretical models. By tuning the $CdSe_{1-x}Te_x$ film composition we are able to vary the optical bandgap from 1.486 eV to 1.677 eV Fitting our results to this equation yields a bowing parameter of 0.88 eV, in good agreement with literature values which vary from 0.59 to 0.91 eV. [36, 37].

Table 3. Values of the Cauchy coefficient parameters (a, b), energy gap E_g^{opt}, width of localized states E_e, the single oscillator energy E_o, the dispersion energy parameter E_d, the linear refractive index n_o, zero-frequency dielectric constant ε_o and moments of the optical spectrum for $CdSe_{1-x}Te_x$ thin films with (x = 0, 0.2, 0.4, 0.6, 0.8 and 1 at. %).

M_{-3}	M_{-1}	ε_o	n_o	E_d (eV)	E_o (eV)	E_g^{opt} (eV)	Cauchy coefficient		Sample
							$b\times10^5$ (nm)^2	a	
0.287	3.32	4.32	2.07	11.28	3.39	1.677	2.63	2.08	**CdSe**
0.324	3.06	4.06	2.01	9.43	3.07	1.565	2.22	2.16	**$CdSe_{0.8}Te_{0.2}$**
0.308	2.90	3.90	1.97	8.90	3.06	1.480	2.49	2.20	**$CdSe_{0.6}Te_{0.4}$**
0.295	2.75	3.75	1.93	8.40	3.05	1.412	2.52	2.25	**$CdSe_{0.4}Te_{0.6}$**
0.319	3.24	4.24	2.06	10.36	3.19	1.418	2.76	2.19	**$CdSe_{0.2}Te_{0.8}$**
0.310	3.53	4.53	2.12	11.92	3.37	1.486	2.96	2.17	**CdTe**

3.2.4. Evaluation of the dispersion parameters

According to the single oscillator model proposed by wimple and DiDomenico [38, 39], The data of the dispersion of the refractive index, n were evaluated as:

$$(n^2-1)^{-1}=\frac{E_o}{E_d}-\frac{1}{E_oE_d}(h\nu)^2 \tag{10}$$

where, E_o is the oscillator energy and E_d is the dispersion energy parameter. Fig. 9 plots $(n^2\text{-}1)^{-1}$ versus $(h\nu)^2$ for the investigated thin films. The E_d and E_o were directly determined from the slopes $(E_oE_d)^{-1}$ and the intersection of the straight lines (E_o/E_d) at the vertical axis.

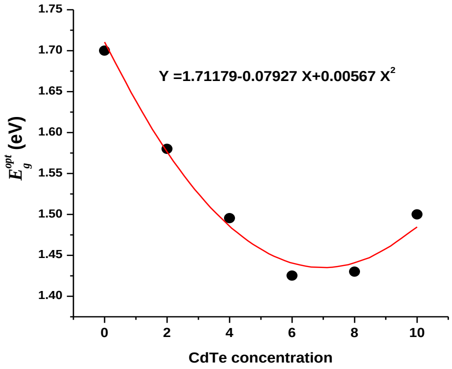

Fig. 9. Energy gap against Co content of $Zn_{1-x}Co_xSe$ *thin films.*

The obtained values of E_o and E_d are presented in Table 3. The values of E_d and E_o decrease with increasing Te content of the investigated films and then increase. The obtained values of E_o are in proportion to the Tauc band gap, E_g as $E_o \approx 2E_g^{opt}$ [40]. On the other hand, a measure of inter-band transition strengths can be provided from the M_{-1} and M_{-3} moments of the optical spectrum. The M_{-1} and M_{-3} moments can be computed as [41]:

$$M_{-1}=\frac{E_d}{E_o}, \quad M_{-3}=\frac{E_d}{E_o^3} \tag{11}$$

Furthermore, using the dispersion and oscillator parameters allow to compute the static refractive index as:

$$n_o=(1+E_d/E_0)^{1/2} \tag{12}$$

The obtained values of M_{-1}, M_{-3} and n_o are listed in Table 3. Thus, the values of zero-frequency dielectric constant $\varepsilon_o = n_o^2$ were calculated. The values of the n_o and ε_o for all the investigated films are determined and listed in Table 3. The values of n_o and ε_o decrease with the increasing Te content (in the first four samples) then increase (in the final two samples).

3.2.5. Evaluation of the non-linear refractive index

The nonlinear refractive index, n_2 was deduced in terms of Tichy and Ticha relationship [42]. Tichy and Ticha relationship is a combination of Miller's popularized rule and static refractive index computed from WDD model as [43]:

$$n_2=\left[\frac{12\pi}{n_o}\right]\chi^{(3)} \tag{13}$$

where $\chi^{(3)}$ is third order non-linear susceptibility and computed from the following relation [44]:

$$\chi^{(3)} = A[\chi^{(1)}]^4 \tag{14}$$

where $\chi^{(1)}$ is linear susceptibility which is expressed as:

$$\chi^{(1)} = \frac{1}{4\pi}\left[\frac{E_d}{E_o}\right] \tag{15}$$

where A = 1.7×10^{-10} (for $\chi^{(3}$ in esu). Therefore, $\chi^{(3)}$ is expressed as:

$$\chi^{(3)} = \frac{A}{(4\pi)^4}\left(n_o^2 - 1\right)^4 \tag{16}$$

It is found that the value of the nonlinear refractive index increases with increasing Te content of investigated samples then decreases. Fig. 10 plots the non-linear refractive index according to Tichy and Ticha relationship versus wavelength.

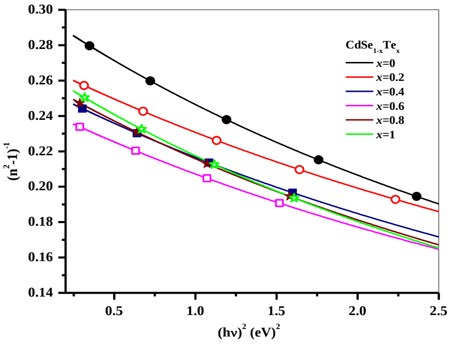

Fig. 10. The plot of $(n^2-1)^{-1}$ vs. $(h\nu)^2$ for $CdSe_{1-x}Te_x$ thin films with (x = 0, 0.2, 0.4, 0.6, 0.8 and 1 at. %).

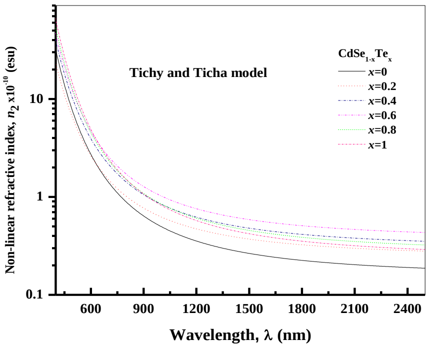

Fig. 11. The dependence of non-linear refractive index according to Tichy and Ticha model on the for $CdSe_{1-x}Te_x$ thin films with (x = 0, 0.2, 0.4, 0.6, 0.8 and 1 at. %).

4. Conclusions

Polycrystalline materials of $CdSe_{1-x}Te_x$ with (x = 0, 0.2, 0.4, 0.6, 0.8 and 1 at. %) were prepared by a conventional solid-state reaction method. Thin films of $CdSe_{1-x}Te_x$ of about 0.5 μm have been produced using evaporation method technique. X–ray diffraction has been used to emphasize the crystalline nature of these samples that well oriented along a preferred direction of

(002) for hexagonal and along (111) for cubic crystal structure. The envelop method has been introduced to find the film thickness, refractive index, and hence other optical parameters. The change values of *n* was related to the change in the concentration of Te to the expense of Se content.

The optical band gap was determined from absorption spectra of the films in the high absorption region. The band gap displays allowed direct transition and decreases from 1.7 eV (CdSe) with an increase in Te concentration passing through a minimum of 1.41 eV for $CdSe_{0.4}Te_{0.6}$ (x = 0.6) and then for higher Te concentration band gap increases to 1.5 eV corresponds to pure CdTe. It is observed that the variation in the band gap with composition exhibits band gap bowing in a quadratic form. The dispersion of the refractive index studied utilizing the WDD single oscillator model. The nonlinear refractive index of Cd-Se-Te films is well correlated with the linear refractive index and WDD parameters.

Acknowledgments

This work was support of King Khalid University, the Ministry of Education, and Kingdom of Saudi Arabia for this research through a grant (RCAMS/KKU/005/20) under research center for advanced material science.

References

[1] M. A. Green, K. Emery, Y. Hishikawa, W. Warta, E. D. Dunlop, D. H. Levi, A. W. Y. Hobaillie, Prog. Photovolt. Res. Appl. **25**, 3 (2017).
[2] D. E. Swanson, J. R. Sites, W. S. Sampath, Sol. Energy Mater. Sol. Cells **159**, 389 (2017).
[3] X. Wu, Sol. Energy **77**, 803 (2004).
[4] N. R. Paudel, Y. Yan, Appl. Phys. Lett. **105**, 183510 (2014).
[5] A. A. Taylor, J. D. Major, G. Kartopu, D. Lamb, J. Duenow, R. G. Dhere, X. Maeder, S. J. C. Irvine, K. Durose, B. G. Mendis, Sol. Energy Mater. Sol. Cells **141**, 341 (2015).
[6] N. Romeo, A. Bosio, V. Canevari, A. Podestà, Sol. Energy **77**, 795 (2004).
[7] J. M. Kephart, J. W. McCamy, Z. Ma, A. Ganjoo, F. M. Alamgir, W. S. Sampath, Sol. Energy Mater. Sol. Cells **157**, 266 (2016).
[8] J. D. Poplawsky, W. Guo, N. Paudel, A. Ng, K. More, D. Leonard, Y. Yan, Nat. Commun. **7**, (2016).
[9] A. Munshi, J. Kephart, A. Abbas, J. Raguse, J. Beaudry, K. Barth, J. Walls, W. Sampath, Proceedings of the 44th IEEE Photovoltaics Specialists Conference Washinton D.C., 2017.
[10] A. Klein, J. Phys. Condens. Matter **27**, 1 (2015).
[11] J. D. Major, Y. Y. Proskuryakov, K. Durose, G. Zoppi, I. Forbes, Sol. Energy Mater. Sol. Cells **94**, 1107 (2010).
[12] J. D. Major, R. E. Treharne, L. J. Phillips, K. Durose, Nature **511**, 334 (2014).
[13] J. Perrenoud, L. Kranz, C. Gretener, F. Pianezzi, S. Nishiwaki, S. Buecheler, A. N. Tiwari, J. Appl. Phys. **114**, 1 (2013).
[14] A. Almohammedi, A. Ashoura, E. R. Shaaban, Chalcogenide Letters **15**, 555 (2018).
[15] E. R. Shaaban, I. Kansal, S. Mohamed, S. Ferreira, Physica B: Condensed Matter **404**, 3571 (2009).
[16] E. R. Shaaban, J. Alloys Compd. **563**, 274 (2013).
[17] J. Zhang, L. Feng, W. Cai, J. Zheng, Y. Cai, B. Li, L. Wu, Y. Shao, Thin Solid Films **414**, 113 (2002).
[18] B. D. Cullity, Elements of X-ray Diffraction: Addison-Wesley Publishing Company, 1978.
[19] E. Márquez, E. R. Shaaban, A. M. Abousehly, Int. J. New. Hor. Phys **1**, 17 (2014).
[20] E. R. Shaaban, M. A. Kaid, M. G. S. Ali, Journal of alloys and compounds **613** 324 (2014).
[21] R. Swanepoel, J. Phys. E: Sci. Instrum. **17**, 896 (1984).
[22] E. R. Shaaban, Y. A. M. Ismail, H. S. Hassan, Journal of non-crystalline solids **376** 61(2013).

[23] P. Sharma, S. C. Katyal, J. Appl. Phys. **107**, 113527 (2010).
[24] E. Márquez, J. M. González-Leal, A. M. Bernal-Oliva, R. Jiménez-Garay, T. Wagner, Journal of Non-Crystalline Solids **354**, 503 (2008).
[25] E. R. Shaaban, M. N. Abd-el Salam, M. Mohamed, M. A. Abdel-Rahim, A. Y. Abdel-Latief, Journal of Materials Science: Materials in Electronics **28**, 13379 (2017).
[26] E. R. Shaaban, M. M. Mahasen, M. M. Soraya, E. S. Yousef, S. A. Mahmoud, G. A. Ali, H. A. Elshaikh, J. Am. Ceram. Soc. **102**, 4067 (2019).
[27] E. R. Shaaban, I. S.Yahia, N. Afify, G. F.Salem, W. Dobrowolski, Materials Science in Semiconductor Processing **19**, 107 (2014).
[28] E. A. Davis, N. F. Mott, Philos. Mag. **22**, 903 (1970).
[29] M. Kastner, Physical. Review Letter **28**, 355 (1972)
[30] E. A. Davis, N. F. Mott, Philos. Mag. **22**, 903 (1970).
[31] J. Tauc, Amorphous and liquid semiconductors, New York: Plenum Press, 1979. p. 159.
[32] B. E. McCandless, J. R. Sites, Cadmium Telluride Solar Cells. In Handbook of Photovoltaic Science and Engineering, 2nd ed.; Luque, A., S., H., Ed.; John Wiley & Sons: New York, 2011.
[33] J. Van Vechten, T. Bergstresser, Electronic Structures of Semiconductor Alloys. Phys. Rev. B **1**, 3351 (1970).
[34] Z. C.; Feng, P. Becla, L. S. Kim, S. Perkowitz, Y. P. Feng, H. C.; Poon, K. P. Williams, G. D Pitt., J. Cryst. Growth **138**, 239 (1994).
[35] L. Hannachi, N. Bouarissa, Superlat. Microstruct. **44**, 794 (2008).
[36] N. El-Kabnay, E. R. Shaaban, N. Afify, A. M. Abou-Sehly, Physica B: Condensed Matter **403** (1), 31 (2008)
[37] R. Islam, H. D. Banerjee, D. R. Rao, Thin Solid Films **266**, 215 (1995).
[38] F. Yakuphanoglu, A. Cukurovali, I. Yilmaz, Optical Materials **27**, 1363 (2005).
[39] S. Wemple, Physical Review B **7**, 3767 (1973).
[40] K. Tanaka, Thin Solid Films **66**, 271 (1980).
[41] F. Yakuphanoglu, A. Cukurovali, İ. Yilmaz, Physica B: Condensed Matter **353**, 210 (2004).
[42] H. Ticha, L. Tichy, J. Optoelectron. Adv. M. **4**, 381 (2002).
[43] E. R. Shaaban, M. M. Mahasen, M. M. Soraya, E. S. Yousef, S. A. Mahmoud, G. A. M. Ali, H. A. Elshaikh, Journal of the American Ceramic Society, (2018).
[44] C. C. Wang, Physical Review B **2**, 2045 (1970).